



Published in final edited form as:

Hum Mutat. 2016 August ; 37(8): 727–731. doi:10.1002/humu.22998.

A Homozygous *Nme7* Mutation Is Associated with *Situs Inversus Totalis*

Orit Reish^{1,2,†,‡}, Liam Aspit^{3,‡}, Arielle Zouella³, Yehudah Roth^{2,4}, Sylvie Polak-Charcon⁵, Tatiana Baboushkin^{2,5}, Lilach Benyamini¹, Todd E. Scheetz⁶, Huda Mussaffi^{2,7}, Val C. Sheffield⁸, and Ruti Parvari^{3,9,*}

¹Genetic Institute, Assaf Harofeh Medical Center, Zerifin, Israel

²The Sackler School of Medicine, Tel Aviv University, Tel Aviv, Israel

³Shraga Segal Department of Microbiology, Immunology and Genetics, Faculty of Health Sciences, Ben-Gurion University of the Negev, Beer Sheva, Israel

⁴Department of Otolaryngology – Head and Neck Surgery, Edith Wolfson Medical Center, Holon, Israel

⁵Department of Pathology, The Sheba Medical Center at Tel Hashomer, Ramat Gan, Israel

⁶Stephen A Wynn Institute for Vision Research and Department of Ophthalmology and Visual Sciences, University of Iowa, Iowa City, Iowa

⁷Pediatric Pulmunology Institute, Schneider Children's Medical Center of Israel, Petach Tikva, Israel

⁸Department of Pediatrics, Division of Medical Genetics, University of Iowa, Iowa City, Iowa

⁹National Institute of Biotechnology in the Negev, Ben-Gurion University of the Negev, Beer Sheva, Israel

Abstract

We investigated the cause of *situs inversus totalis* (SIT) in two siblings from a consanguineous family. Genotyping and whole-exome analysis revealed a homozygous change in *NME7*, resulting in deletion of an exon causing an in-frame deletion of 34 amino acids located in the second NDK domain of the protein and segregated with the defective lateralization in the family. *NME7* is an important developmental gene, and NME7 protein is a component of the γ -tubulin ring complex. This mutation is predicted to affect the interaction of NME7 protein with this complex as it deletes the amino acids crucial for the binding. SIT associated with homozygous deletion in our patients is in line with *Nme7*^{-/-} mutant mice phenotypes consisting of congenital hydrocephalus and SIT, indicating a novel human laterality patterning role for NME7. Further cases are required to elaborate the full human phenotype associated with *NME7* mutations. *Hum Mutat* 0:1–5, 2016.

[†]Correspondence to: Orit Reish, Genetic Institute, Assaf Harofeh Medical Center, Zerifin 70300, Israel. oreish@post.tau.ac.il.

^{*}Correspondence to: Ruti Parvari, Shraga Segal Department of Microbiology, Immunology and Genetics, Faculty of Health Sciences and National Institute of Biotechnology in the Negev, Ben Gurion University of the Negev, Beer Sheva 84105, Israel. ruthi@bgu.ac.il.

[‡]Equal contribution.

Keywords

NME7; γ -tubulin ring complex; cilia; *situs inversus totalis*

The human body, although bilaterally symmetrical in appearance, shows a considerable left–right asymmetry involving many internal organs in their position and shape. Complete mirror-image reversal of this arrangement is called *situs inversus totalis* (SIT) and is estimated to affect about 0.3:10,000 live births [Lin et al., 2014]. SIT is frequently associated with primary ciliary dyskinesia (PCD) [Tabin, 2006], in agreement with the knowledge that visceral asymmetry is determined through embryonic ciliary motion and normal function of the motile cilia plays a key role in the patterning of left–right asymmetry [Fliegauf et al., 2007]. Not all reversals are complete, and a spectrum of intermediate defects (*situs ambiguus*) exists. *Situs ambiguus* includes heterotaxy syndrome (HS) that refers to discordance between asymmetry of different visceral organs, including the heart, lungs, liver, spleen, and stomach. The organs are oriented randomly with respect to the left–right axis and with respect to one another [Srivastava, 1997]. SIT and HS may be part of a phenotypic continuum, caused by the same genetic defects. Variants in the *ZIC3* (MIM# 300265), *CCDC11* (MIM# 614759), or *WDR16* (MIM# 609804) genes were found to cause SIT as well as HS [Ware et al., 2004]. Over 6% of PCD patients were found to have HS [Kennedy et al., 2007], and about half of 43 patients with HS were found to have PCD [Nakhleh et al., 2012]. Variants in only a few genes are currently known to cause isolated, nonsyndromic laterality defects like *MMP21* (MIM# 608416) and *Nodal* (MIM# 601265) in which mutations account for about 5.9% and 5% of HS patients, respectively [Guimier et al., 2015; Mohapatra et al., 2009], *ZIC3* affecting 1% [Ware et al., 2004], the Activin receptor, *ACVR2B* (MIM# 602730) [Kosaki et al., 1999], *CFC1* (MIM# 115150) [Bamford et al., 2000], *SHROOM3* (MIM# 604570) [Tariq et al., 2011], each present in only a minority of HS patients. Here we present another player in left–right asymmetry patterning, identified through genotyping and exome analysis in two siblings from a consanguineous family who presented with SIT. One sibling has severe milk allergy and sinopulmonary symptoms. Cilia from both siblings demonstrated normal ciliary structure and function. Further cases in the future will be able to elaborate on the pulmonary impact of mutation of this gene.

The study was approved by the Assaf Harofe Medical Center institutional review board, and all participants gave written informed consent prior to participation. Parents were first cousins once removed of Muslim origin, had one healthy and two affected off springs, 21 and 6 years old, male and female, respectively (Fig. 1A). SIT was determined in both, following chest X-rays, echocardiography, and abdominal ultrasound. Patient II-1 has no sinopulmonary symptoms; patient II-2 has a small ventricular septal defect with spontaneous closure. She additionally has severe milk allergy with anaphylaxis reaction and respiratory symptoms including intermittent rhinitis, wheezing, dry cough, and several chest infections which were resolved with oral antibiotics and inhaled bronchodilators. Chest CT and sperm motility were not performed. Cilia derived from nasal brushing from both siblings demonstrated heterogeneous alterations (Supp. Fig. S1) and normal ciliary beat frequency and pattern by high-speed video microscopy. Nasal nitric oxide level and spirometry performed on patient II-2 were normal (Supp. Table S1).

Assuming homozygosity by descent of a recessive mutation as the likely cause of the disorder, we have genotyped the patients (Fig. 1A); II-1, II-2) and both parents (see Supp. Methods). We identified six autozygosity regions larger than 3 cM, shared by the two patients encompassing a total of 77.56 Mbp (70.5 cM). Exome sequencing was performed on Patient II-1 (see Supp. Methods). Eight homozygous variations with allele frequency of less than 1% in the public databases (ExAc browser, 1000 Genomes, dbSNP, Exome Variant Server) were identified in the autozygosity regions shared by the two patients (Supp. Table S2). Of these variations, two appeared at a frequency of 1.4% and 2.5% in our Bedouin-Muslim exome database. Five additional variations were excluded because they had a low prediction of being damaging using the Omicia score, which is based on six prediction programs (Mutation Taster, Polyphen-2, SIFT, Phylo-P of three comparisons and additionally by VVP and CADD). The only remaining variation: chr1: 169199951C > T (hg19/GRCh37), NM 013330.3:c.990 + 5G > A in intron 10 of *Nme7* (expressed in nonmetastatic cell 7; MIM# 613465) present in the largest autozygosity region of 31.7cM (23.6Mb) was further considered. This variant is novel, not reported in the public databases, segregates as expected in the family, namely it is found to be homozygous in the patients and heterozygous in the parents and the healthy sibling (Fig. 1A, B). Individuals with a homozygous defect in *NME7* are expected to have random lateralization (50% of individuals with SIT and 50% with a normal phenotype), thus it is possible that a normal individual could be homozygous for the mutation; however, patients with complete *situs inversus* would be expected to be homozygous for the mutation as observed in the family. The variant was excluded as a population-specific variation by not being present in 83 control Bedouin-Muslims of the Negev, composed of our Bedouin exome collection and samples that were analyzed by restriction analysis with *TasI*, a site created by the variation (Fig. 1A).

Since the BDGP splice prediction program predicted that the variation would be detrimental to the donor splice site, we directly verified the effect of the gene variant on the splicing. RNA was extracted from lymphoblastoid cells that were established from the two patients, their mother and from comparable cells of control individuals, and cDNA was prepared. PCR was performed on the cDNA using primers in exons 8 and 12, flanking intron 10 that contains the mutation. The RT-PCR products of the patient-derived cells demonstrate a faster migrating band in contrast to the expected fragment of normal splicing shown in control cells and two bands in the mother, of the patient and control sizes (Fig. 1C). Sanger sequencing of the PCR products demonstrated that the small fragment of the patients (295 bp) is missing in exon 10 whereas the large fragment of the control (397 bp) shows the expected splicing (Fig. 1D).

NME7 has an N-terminal DM10 domain, which consists of approximately 105 residues whose function is unknown. This domain has been identified in only two types of proteins: nucleoside diphosphate kinases (which contain a single copy of the DM10 domain) and in an uncharacterized class of proteins (which contain multiple copies of DM10 domains) (Uniprot). The protein also contains two nucleoside diphosphate kinase (NDPK) domains (Fig. 2A), but both domains lack the residues deemed crucial for enzyme structure and activity (reviewed in [Desvignes et al., 2009]). Yoon et al. [Yoon et al., 2005] confirmed the lack of kinase activity in human *NME7* but reported a marked exonuclease activity. The DM10 domain may act as a flagellar NDPK regulatory module or as a unit specifically

involved in axonemal targeting or assembly [King, 2006]. *NME7* has two coding splice variants, which differ in the second exon and the start of translation; the second variant misses the 36 N-terminal amino residues and thus part of the DM10 domain [Kallberg et al., 2012], thus the skipping of exon 10 will affect both known splice variants. The skipping of exon 10 causes an in-frame deletion of 34 amino acids that are highly conserved in the second NDK domain (Fig. 2A, B). Using RaptorX Webserver, the three-dimensional structure of *NME7* protein was modeled with the orthorhombic crystal form *C222* of the *Aquifex aeolicus* nucleoside diphosphate kinase that represents the most similar known structure. The 34 amino acids that are deleted by the mutation are correspondent to the removal of the central beta sheet and two adjacent alpha helices, thus predicted to unfold the NDK2 domain (Fig. 2C). We have verified the RNA expression pattern of *NME7* on eight adult human organs by quantitative RT-PCR using commercially available RNA and found that it is ubiquitously expressed and abundantly expressed in brain and testis (Supp. Fig. S2).

The left–right axis is established in early embryonal stages, subsequent to the development of anterior–posterior and dorsal–ventral axes. According to the generally accepted model, the initiation of asymmetry is coordinated by nodal cilia, which create leftward flow [Tabin, 2006]. The flow forms a concentration gradient detected by sensory immotile cilia producing intracellular signal transduction [Yoshida et al., 2012]. This nodal signaling pathway activates an asymmetric developmental program in visceral primordial cells within the lateral plate mesoderm [Yoshida et al., 2012]. Nodal cilia share many structural features with other motile cilia, and impaired function of the nodal cilia is likely an integral part of primary cilia dyskinesia (PCD; MIM# 244400), in which situs is randomized.

NME7 is one of 10 genes in human that belong to the NME family (previously known as Nm23 or nucleoside diphosphate kinase (NDPK)). Vertebrate *Nme* genes can be separated in two evolutionary distinct groups. *Nme1-4* belong to Group I whereas vertebrate *Nme5-10* belong to Group II. The proteins encoded by group II, except for *NME6*, lack NDPK activity. *NME7* as well as *NME6* (MIM# 608294) are important developmental genes as revealed by a shRNA functional screen for the creation of induced pluripotent embryonic stem cells. Knockdown of either *Nme6* or *Nme7* reduces the formation of embryoid body (EB) and teratoma. The overexpression of either *Nme6* or *Nme7* can rescue the stem cell marker expression and the EB formation in the absence of leukemia inhibiting factor [Wang et al., 2012].

In humans, *NME7* is predominantly expressed in testis and at significant levels in ovary and brain (Supp. Fig. S2 and [Lacombe et al., 2000]). Western blotting analyses of various mouse tissues consistently indicated that it is preferentially expressed in tissues with motile cilia as well as in sperm. Immunofluorescence microscopy revealed that this protein is localized along the entire length of the TritonX-100-insoluble fraction of sperm flagella, possibly in the axonemes. Additionally, in vitro cosedimentation assays using recombinant proteins showed that both mouse and *Chlamydomonas NME7* directly bind to microtubules [Ikeda, 2010]. Moreover, in three cell lines siRNA to *NME7* demonstrated that knockdown of *NME7* causes transport and signaling defects in cilia yet retained normal looking cilia. Since depletion of *NME7* also accumulates putative secretory transport vesicles and

decreases ciliary levels of GPCRs, it was speculated that *NME7* may regulate vesicular transport from the Golgi to the plasma membrane [Lai et al., 2011].

In a systematic analysis of human proteins involved in chromosome segregation *NME7* was identified as a component of the γ -tubulin ring complex (γ TuRC) [Hutchins et al., 2010]. It was also found in this complex by interaction with CDK5RAP2, a human microcephaly protein that binds the complex and is involved in centrosomal attachment of γ -tubulin [Choi et al., 2010]. Finally, *NME7* interacts with the γ TuRC through both NDK domains, with Arg-322 in the second NDK domain being crucial to the binding [Liu et al., 2014]. The 34 amino acids predicted to be deleted by the mutation we identified, including Arg at position 322, are missing in the mutated protein (Fig. 2B). This deletion is expected to have a deleterious effect on the interaction between *NME7* and γ TuRC.

The probable role of *NME7* in cilia is revealed by the presentations of mice knocked out for this gene. A high-throughput study of mutagenesis and phenotyping process designed to characterize protein functions demonstrated that knock out of *Nme7* by gene trap caused congenital hydrocephalus in almost 100% of *Nme7*^{-/-} mice, *situs inversus* in 50%, but neither infertility nor severe rhinosinosis was detected [Vogel et al., 2010, 2012]. However, other members of the NME group II family *Nme5* [Vogel et al., 2012] and *NME8* (MIM# 607421) [Duriez et al., 2007] have been involved in nasal exudates in mice and PCD in human, respectively. It was suggested that the function and biogenesis of motile cilia/flagella in the respiratory epithelium and spermatozoa are less dependent on functional NDP kinase 7 than are the motile cilia of embryonic node. Also, the phenotypic difference between *Nme5*^{-/-} and *Nme7*^{-/-} mice may illustrate that there is structural and functional variation in motile cilia at different locations [respiratory epithelium and embryonic node, Vogel et al., 2012].

The two patients reported here are not sufficient for genotype–phenotype correlation. On the one hand, they do not have congenital hydrocephalus, previously associated with ventricular motile cilia abnormalities [Chamling et al., 2013] and consistent with hydrocephalus in *Nme7*^{-/-} mice. On the other hand, both patients lacked objective evidence of ciliary dysfunction in line with the findings in mutant mice. Ciliary ultrastructure, ciliary beat frequency, and pattern were normal. Although patient II-2 has atopy and milk allergy that may explain her respiratory symptoms, we cannot rule out some ciliary dysfunction in vivo and in certain condition such as viral infections.

Since *NME7* has not been previously characterized in humans, further cases in the future may elaborate the phenotypic impact of this gene.

We conclude that a deleterious mutation in *NME7*, which results in deletion of amino acids necessary for its interaction with the γ TuRC is associated with impaired left–right asymmetry manifested by SIT. The phenotypic spectrum of the reported mutation cannot be fully characterized based on the present small sample size and should be determined in the future.

Supplementary Material

Refer to Web version on PubMed Central for supplementary material.

Acknowledgments

We are most grateful to Dr. Raz Zarivach from the Department of Life Sciences of Ben Gurion University of the Negev for his expert contribution to the three-dimensional modeling of the protein and the parts affected by the mutation.

Contract grant sponsors: United States-Israel Binational Science Foundation (2011460).

References

- Bamford RN, Roessler E, Burdine RD, Saplakoglu U, dela Cruz J, Splitt M, Goodship JA, Towbin J, Bowers P, Ferrero GB, Marino B, Schier AF, Shen MM, Muenke M, Casey B. Loss-of-function mutations in the EGF-CFC gene CFC1 are associated with human left-right laterality defects. *Nat Genet.* 2000; 26:365–369. [PubMed: 11062482]
- Chamling X, Seo S, Bugge K, Searby C, Guo DF, Drack AV, Rahmouni K, Sheffield VC. Ectopic expression of human BBS4 can rescue Bardet-Biedl syndrome phenotypes in Bbs4 null mice. *PLoS One.* 2013; 8:e59101. [PubMed: 23554981]
- Choi YK, Liu P, Sze SK, Dai C, Qi RZ. CDK5RAP2 stimulates microtubule nucleation by the gamma-tubulin ring complex. *J Cell Biol.* 2010; 191:1089–1095. [PubMed: 21135143]
- Desvignes T, Pontarotti P, Fauvel C, Bobe J. Nme protein family evolutionary history, a vertebrate perspective. *BMC Evol Biol.* 2009; 9:256. [PubMed: 19852809]
- Duriez B, Duquesnoy P, Escudier E, Bridoux AM, Escalier D, Rayet I, Marcos E, Vojtek AM, Bercher JF, Amselem S. A common variant in combination with a nonsense mutation in a member of the thioredoxin family causes primary ciliary dyskinesia. *Proc Natl Acad Sci U S A.* 2007; 104:3336–3341. [PubMed: 17360648]
- Fliegauf M, Benzing T, Omran H. When cilia go bad: cilia defects and ciliopathies. *Nat Rev Mol Cell Biol.* 2007; 8:880–893. [PubMed: 17955020]
- Guimier A, Gabriel GC, Bajolle F, Tsang M, Liu H, Noll A, Schwartz M, El Malti R, Smith LD, Klena NT, Jimenez G, Miller NA, et al. MMP21 is mutated in human heterotaxy and is required for normal left-right asymmetry in vertebrates. 2015; 47:1260–1263.
- Hutchins JR, Toyoda Y, Hegemann B, Poser I, Heriche JK, Sykora MM, Augsburg M, Hudecz O, Buschhorn BA, Bulkescher J, Conrad C, Comartin D, et al. Systematic analysis of human protein complexes identifies chromosome segregation proteins. *Science.* 2010; 328:593–599. [PubMed: 20360068]
- Ikeda T. NDP kinase 7 is a conserved microtubule-binding protein preferentially expressed in ciliated cells. *Cell Struct Funct.* 2010; 35:23–30. [PubMed: 20215702]
- Kallberg M, Wang H, Wang S, Peng J, Wang Z, Lu H, Xu J. Template-based protein structure modeling using the RaptorX web server. *Nat Protoc.* 2012; 7:1511–1522. [PubMed: 22814390]
- Kennedy MP, Omran H, Leigh MW, Dell S, Morgan L, Molina PL, Robinson BV, Minnix SL, Olbrich H, Severin T, Ahrens P, Lange L, et al. Congenital heart disease and other heterotaxic defects in a large cohort of patients with primary ciliary dyskinesia. *Circulation.* 2007; 115:2814–2821. [PubMed: 17515466]
- King SM. Axonemal protofilament ribbons, DM10 domains, and the link to juvenile myoclonic epilepsy. *Cell Motil Cytoskeleton.* 2006; 63:245–253. [PubMed: 16572395]
- Kosaki R, Gebbia M, Kosaki K, Lewin M, Bowers P, Towbin JA, Casey B. Left-right axis malformations associated with mutations in ACVR2B, the gene for human activin receptor type IIB. *Am J Med Genet.* 1999; 82:70–76. [PubMed: 9916847]
- Lacombe ML, Milon L, Munier A, Mehus JG, Lambeth DO. The human Nm23/nucleoside diphosphate kinases. *J Bioenerg Biomembr.* 2000; 32:247–258. [PubMed: 11768308]

- Lai CK, Gupta N, Wen X, Rangell L, Chih B, Peterson AS, Bazan JF, Li L, Scales SJ. Functional characterization of putative cilia genes by high-content analysis. *Mol Biol Cell*. 2011; 22:1104–1119. [PubMed: 21289087]
- Lin AE, Krikov S, Riehle-Colarusso T, Frias JL, Belmont J, Anderka M, Geva T, Getz KD, Botto LD. Laterality defects in the national birth defects prevention study (1998–2007): birth prevalence and descriptive epidemiology. *Am J Med Genet A*. 2014; 164a:2581–2591. [PubMed: 25099286]
- Liu P, Choi YK, Qi RZ. NME7 is a functional component of the gamma-tubulin ring complex. *Mol Biol Cell*. 2014; 25:2017–2025. [PubMed: 24807905]
- Mohapatra B, Casey B, Li H, Ho-Dawson T, Smith L, Fernbach SD, Molinari L, Niesh SR, Jefferies JL, Craigen WJ, Towbin JA, Belmont JW, Ware SM. Identification and functional characterization of NODAL rare variants in heterotaxy and isolated cardiovascular malformations. *Hum Mol Genet*. 2009; 18:861–871. [PubMed: 19064609]
- Nakhleh N, Francis R, Giese RA, Tian X, Li Y, Zariwala MA, Yagi H, Khalifa O, Kureshi S, Chatterjee B, Sabol SL, Swisher M, et al. High prevalence of respiratory ciliary dysfunction in congenital heart disease patients with heterotaxy. *Circulation*. 2012; 125:2232–2242. [PubMed: 22499950]
- Srivastava D. Left, right... which way to turn? *Nat Genet*. 1997; 17:252–254. [PubMed: 9354777]
- Tabin CJ. The key to left-right asymmetry. *Cell*. 2006; 127:27–32. [PubMed: 17018270]
- Tariq M, Belmont JW, Lalani S, Smolarek T, Ware SM. SHROOM3 is a novel candidate for heterotaxy identified by whole exome sequencing. *Genome Biol*. 2011; 12:R91. [PubMed: 21936905]
- Vogel P, Read R, Hansen GM, Freay LC, Zambrowicz BP, Sands AT. Situs inversus in *Dpcd/Poll*^{-/-}, *Nme7*^{-/-}, and *Pkd111*^{-/-} mice. *Vet Pathol*. 2010; 47:120–131. [PubMed: 20080492]
- Vogel P, Read RW, Hansen GM, Payne BJ, Small D, Sands AT, Zambrowicz BP. Congenital hydrocephalus in genetically engineered mice. *Vet Pathol*. 2012; 49:166–181. [PubMed: 21746835]
- Wang CH, Ma N, Lin YT, Wu CC, Hsiao M, Lu FL, Yu CC, Chen SY, Lu J. A shRNA functional screen reveals *Nme6* and *Nme7* are crucial for embryonic stem cell renewal. *Stem Cells*. 2012; 30:2199–2211. [PubMed: 22899353]
- Ware SM, Peng J, Zhu L, Fernbach S, Colicos S, Casey B, Towbin J, Belmont JW. Identification and functional analysis of *ZIC3* mutations in heterotaxy and related congenital heart defects. *Am J Hum Genet*. 2004; 74:93–105. [PubMed: 14681828]
- Yoon JH, Singh P, Lee DH, Qiu J, Cai S, O'Connor TR, Chen Y, Shen B, Pfeifer GP. Characterization of the 3'→5' exonuclease activity found in human nucleoside diphosphate kinase 1 (NDK1) and several of its homologues. *Biochemistry*. 2005; 44:15774–15786. [PubMed: 16313181]
- Yoshida S, Shiratori H, Kuo IY, Kawasumi A, Shinohara K, Nonaka S, Asai Y, Sasaki G, Belo JA, Sasaki H, Nakai J, Dworniczak B, et al. Cilia at the node of mouse embryos sense fluid flow for left-right determination via *Pkd2*. *Science*. 2012; 338:226–231. [PubMed: 22983710]

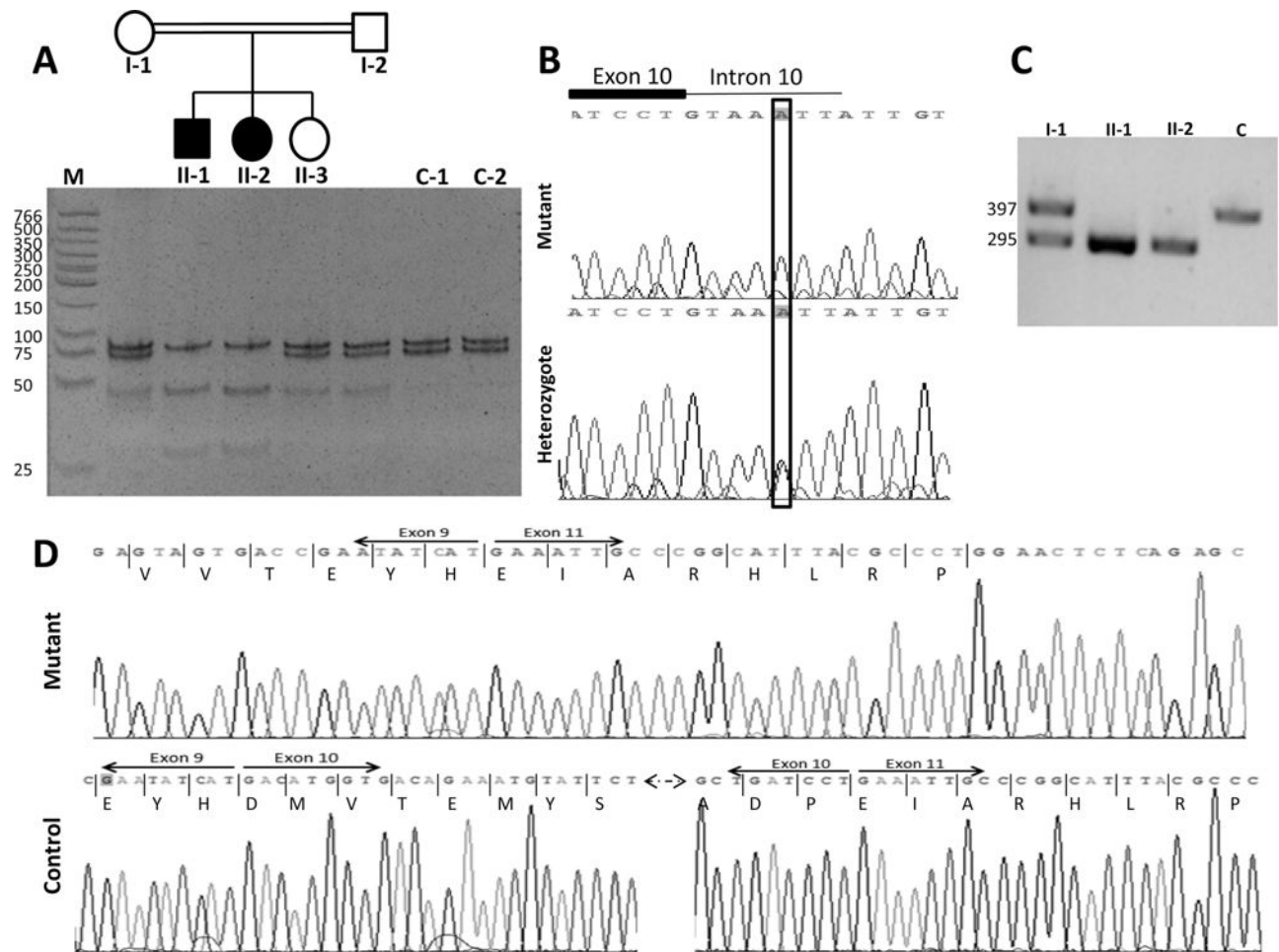


Figure 1.

Family pedigree and identification of the mutation. (A) Pedigree: The segregation of the *NME7* mutation that creates a *TasI* site is shown by restriction analysis, under each individual and two controls. Digestion of the 148 bp amplicon with *TasI* results in 78 and 70 bp fragments in controls. When the mutation is present, the 70 bp fragment is cleaved into 44 and 26 bp fragments. Digestion products were separated by electrophoresis on 20% polyacrylamide gels. The patients are homozygous for the mutation, all available parents and all healthy siblings are heterozygotes, and the controls are homozygous for the normal allele. (B) Sequence chromatogram of PCR product of genomic DNA showing the single variant compatible with being a disease-causing mutation, a change in intron 10. The chromatograms show the homozygous mutant (upper panel) and heterozygous sequences (lower panel). (C) Splicing of the *NME7* gene in patients' cells. RT-PCR products. RNA was extracted from lymphoblastoid cells of the two patients (II-1 and II-2), the mother (I-1) and a control (C). PCR was performed on the cDNA using primers in exons 8 and 12, flanking intron 10 that contains the mutation. PCR products were separated on 2% agarose gels. The patient cells exhibited one fragment of 295 bp in contrast to control cells that had a 397 bp fragment. The heterozygous mother has the two bands. (D) Sequence chromatogram of the 295 bp PCR product of the patients showing the skipping of exon 10 (exon 9 joining directly

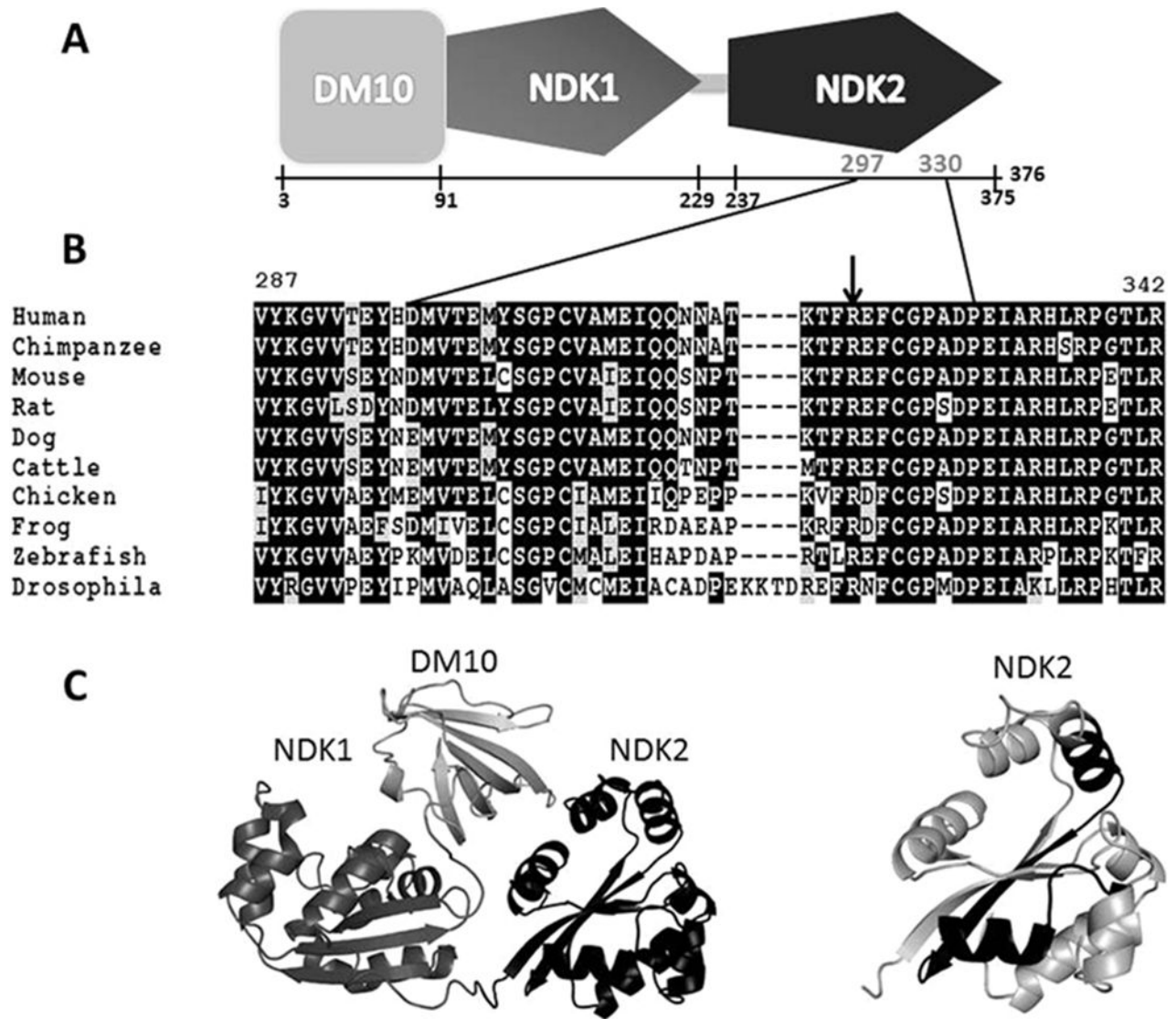
to exon 11) (upper). The 397-bp PCR product shows normal splicing (lower). The mutation was submitted to a *NME7* variant database (<http://www.lovd.nl/NME7>).

Author Manuscript

Author Manuscript

Author Manuscript

Author Manuscript

**Figure 2.**

Effect of the mutation on the protein. (A) Diagram of protein domains and the location of the mutation. The DM10 and NDPK domains are based on the predictions of SMART (Uniprot). The numbering of the amino acids corresponds to the protein produced by splice variant 1, variant 2 misses the 36 amino acids at the N terminus and thus its DM10 domain is not complete. (B) Sequence conservation of the amino acids encoded by exon 10: 297–330, that are missing in the patients are presented between the diagonal lines. Arg at position 322, which is crucial for the binding to the γ -tubulin ring complex, is marked by an arrow. (C) Modelling the 3D structure of the normal protein using the RaptorX program with 3ztoA (Orthorhombic crystal form C222 of the Aquifex aeolicus nucleoside diphosphate kinase since it represents the best alignment, the p value for the entire length of 376 residues is $5.92e-07$; <http://www.rcsb.org/pdb/explore/explore.do?structureId=3zto>) as template, left. The protein region deleted by the mutation is within the NDK2 domain from Asp at position 297 to Pro at position 330 is colored black in this domain in the figure at the right.